HHS Public Access

Author manuscript

Biosens Bioelectron. Author manuscript; available in PMC 2026 July 18.

Published in final edited form as:

Biosens Bioelectron. 2026 June 15; 302: 118519. doi:10.1016/j.bios.2026.118519.

Ultrasound-Enabled Refreshable Electrochemical Sensors for Cardiac Biomarker Monitoring

Mayank Garg[a], **Heng Guo**[a], **Myeong Namkoong**[a], **Elizabeth Zhanov**[a], **Connor Malone**[a], **Md Saifur Rahman**[a], **Ayse Akcan-Arikan**[b], **Limei Tian**[a]

[a]Department of Biomedical Engineering, and Center for Remote Health Technologies and Systems, Texas A&M University, College Station, TX 77843, USA.

[b]Department of Pediatrics, Divisions of Critical Care Medicine and Nephrology, Baylor College of Medicine, Texas Children's Hospital, Houston, TX 77030, USA.

Abstract

Cardiac troponin I (cTnI) is the gold-standard biomarker for acute myocardial infarction, yet current laboratory-based high-sensitivity assays require centralized infrastructure, trained personnel, and serial testing, limiting their suitability for real-time or continuous monitoring in resource-limited settings. Point-of-care electrochemical sensors have shown promise for rapid cTnI detection, but their reliance on antibodies as biorecognition elements and redox mediator solutions, and single-use operation restricts practical translation. Here, we report an ultrasound-enabled refreshable electrochemical biosensor for sensitive, stable, and repeatable cTnI monitoring. The device employs a cTnI-specific peptide as the biorecognition element, providing enhanced stability during storage, transport, and operation. Label-free electrochemical impedance spectroscopy quantifies impedance changes upon cTnI binding in body fluids, including serum and saliva, enabling rapid analysis and high sensitivity with electroosmotic enhancement. The sensor achieves a wide dynamic range from 0.031 pg/mL to 1.5 ng/mL for cTnI detection and quantification in 15 minutes. Compared to previously reported electrochemical platforms and conventional laboratory-based high-sensitivity assays, the proposed sensor offers improved analytical performance, as defined by limit of detection, dynamic range, and assay time. Importantly, low-power ultrasound effectively refreshes the sensor by removing bound targets without damaging the peptide, enabling sustained measurements and prolonging sensor lifetime. The demonstrated sensitivity enhancement and refreshability establish a foundation for extending this approach to diverse biomarkers, paving the way for frequent molecular monitoring and early clinical intervention.

Keywords

Ultrasound; Refreshable; Electrochemical biosensor; Cardiac biomarker; Complex biofluids

ltian@tamu.edu .

Introduction

Cardiovascular disease (CVD) is the leading cause of death globally, accounting for an estimated 20 million deaths annually. Among its manifestations, acute myocardial infarction (AMI) is particularly life-threatening, and its clinical management critically depends on rapid and reliable diagnosis(Thygesen et al. 2018). Cardiac troponins, especially cardiac troponin I (cTnI), are recognized as gold-standard biomarkers due to their high specificity and sensitivity for myocardial injury(Apple et al. 2017; Garg et al. 2017; Wang et al. 2020; Welsh et al. 2019). AMI involves a characteristic rise and/or fall of the troponin level over hours and days.(Thygesen et al. 2018) Even small elevations in circulating cTnI levels can serve as early indicators of cardiac injury, underscoring the need for timely and accurate quantification to guide clinical decision-making and improve patient outcomes. Elevated levels of cardiac troponins might not be detected in the serum for up to 4 hours after AMI onset and require serial tests of troponins after the patient's admission(Apple et al. 2017; Keller and Hamm 2019; Keller et al. 2011). Although numerous clinical care advancements in AMI have been enabled by laboratory-based high-sensitivity cTnI assays, these methods still suffer from long turnaround times, reliance on centralized infrastructure, and the need for trained personnel(Westermann et al. 2017). These limitations hinder their deployment in decentralized or resource-limited settings and restrict their applicability for real-time, frequent, or continuous monitoring.

Point-of-care (POC) biosensing platforms have recently emerged as promising tools for early AMI diagnosis via sensitive cTnI detection(Szunerits et al. 2019; Thulin et al. 2023; Tu et al. 2022). Such platforms offer portability, rapid detection, and reduced sample requirements, making them attractive for bedside monitoring and emergency care in hospitals. Numerous electrochemical sensors have been reported for cTnI detection, demonstrating improved sensitivity and reduced assay time. Many of these sensors rely on antibodies as biorecognition elements to provide high sensitivity and specificity(Cen et al. 2021; Das et al. 2021; Feng et al. 2021; Li et al. 2024). Antibodies are prone to degradation during long-term storage, transport, and repeated use(Guo et al. 2022; Li et al. 2021b; Tadepalli et al. 2015; Yin et al. 2020), which poses significant challenges for translating antibody-based biosensors into practical clinical tools in resource-limited settings and wearable applications. This instability undermines assay reproducibility and shelf and operational life for in vitro and in vivo cTnI quantification. To address this challenge, stable biorecognition elements, including aptamer(Chekin et al. 2018; Eshlaghi et al. 2023; Li et al. 2021a; Negahdary et al. 2017), molecularly imprinted polymer(Ma et al. 2017; Mokhtari et al. 2020), and peptide(Wang et al. 2016), have been employed to improve the sensor stability. However, these electrochemical sensors typically rely on measurements in redox mediator solutions, such as ferro/ferricyanide, to quantify cTnI, which restricts their applicability for real-time, in situ sensing. In addition, refreshing electrochemical sensors after cTnI binding remains a significant challenge, hindering their use in frequent and continuous monitoring.

In this work, we present an ultrasound-enabled refreshable electrochemical sensor to detect and quantify cTnI with high sensitivity, specificity, and stability. The sensor utilizes a cTnI-specific peptide as a stable biorecognition element to ensure sensor stability during storage,

transport, and operation. We employ label-free electrochemical impedance spectroscopy (EIS) to quantify impedance changes in response to various cTnI concentrations in body fluids, including human serum and saliva. The alternating current electroosmosis (ACEO) activated by two interdigitated electrodes in situ enhances sensitivity and expands the dynamic range, enabling quantification of cTnI concentrations from 0.031 pg/mL to 1.5 ng/mL in 15 minutes. This represents an improvement in analytical performance relative to previously reported cTnI electrochemical sensors, in terms of detection limit and assay speed. Low-power ultrasound is able to refresh the sensor without damaging the peptide or reducing sensitivity. Additionally, we demonstrate that the sensor can be fabricated on a flexible substrate, facilitating its integration with the curved surface of the human body.

Materials and Methods

Materials

Human Cardiac Troponin I (cTnI) (Recombinant) was purchased from Life Diagnostics, Inc. Anti-cardiac troponin peptides with sequence FYSHSFHENWPSC were procured from GenScript USA Inc. Bovine serum albumin was purchased from Sigma-Aldrich. Interleukin-6 and tumor necrosis factor-α were obtained from R&D Systems. C-reactive protein was procured from Invitrogen. 10X PBS was purchased from Gibco. Silver nitrate, sodium citrate, hydrochloric acid, and sodium hydroxide were purchased from Fisher Scientific. Iron chloride was purchased from Thermo Scientific. Human serum was obtained from Jackson ImmunoResearch Inc. Artificial Human Saliva was obtained from Biochemazone. Type 1 deionized water (18.2 mΩ·cm) used for preparing solutions and washing was produced by the Sartorius Arium Pro Ultrapure water system.

Fabrication of cTnI sensor

We prepared the four terminal devices with microfabrication involving photolithography. E-beam evaporation deposited thin films of 100 nm gold and 5 nm chromium on glass and polyimide substrates. A photoresist (AZ5412E) was spin-coated on the gold-coated glass substrate or gold-coated polymide substrate, followed by baking at 105 °C for 60 sec. After UV exposure in the presence of a mask, the pattern was developed using a developer (AZ726MIF). Gold and chromium etchants defined the pattern of the electrodes. After the photoresist was removed using a stripping agent, the device was thoroughly cleaned with acetone, isopropanol, and distilled water, and blow-dried with N_2 gas. This device was then attached to an anisotropic conductive film (ACF), which was subsequently bonded to a printed circuit board for convenient connection with a potentiostat (Gamry Instruments Reference 620+). The Ag/AgCl reference electrode was prepared by the electrodeposition of silver on the gold surface by immersing the device into a mixture of 2 mM silver nitrate and 100 mM sodium citrate dihydrate aqueous solution, followed by cyclic voltammetry (−0.9 to 0.9 V, 100 mV/sec scan rate) using the potentiostat. After Ag electrodeposition, 0.1 M iron chloride aqueous solution was drop-casted on the silver-coated electrode for 30 sec to convert Ag to Ag/AgCl. The electrodes were thoroughly rinsed with deionized water again and then blown dry. The interdigitated region of the working electrodes was incubated with 100 μg/mL of peptide aqueous solution for 1 hour, followed by rinsing with deionized water and blown dry. To minimize nonspecific binding, the entire device surface was blocked with

3wt% BSA prepared in 1X PBS for 1 hour, followed by rinsing with deionized water and blown dry.

Characterization and sensing performance

Electrochemical impedance spectroscopy (EIS) was performed to characterize the impedance changes after the sensor was functionalized by peptides and blocked with BSA, and after exposure to the cTnI and interfering molecules. The EIS was recorded in the range of 0.1 to 10 kHz at an AC root mean square (RMS) voltage of 10 mV using Reference 620+ Potentiostat, following a previous protocol(Garg et al. 2024). The impedance after each step of functionalization was recorded in 1X PBS (pH 7.4). The cTnI sensor was exposed to various cTnI concentrations (0.02 pg/mL to 1.5 ng/mL) prepared in 10% human serum (human serum diluted in 1X PBS), followed by recording their impedance spectra. The impedance of the blank (10% human serum without cTnI) was also recorded as baseline.

The selectivity of the sensor was evaluated by exposing it to various physiologically relevant interfering molecules, including IL-6 (7 pg/mL), TNF-α (25 pg/mL), and CRP (3 μg/mL). The corresponding impedance change was measured and compared to that induced by 0.5 pg/mL cTnI. The effect of pH on sensor stability was evaluated by first exposing the sensor to different pH conditions (pH 3, 7.4, and 11), and then exposing it to 0.5 pg/mL cTnI. The impedimetric change against the blank was measured and compared. To evaluate the sensor stability, the cTnI sensor was stored in 1X PBS at 37 °C for 1–4 days. The sensor was exposed to 0.5 pg/mL of cTnI concentration to record the impedimetric change against the blank. To test the refreshability of a sensor, the cTnI sensor was exposed to cTnI at a concentration of 0.5 pg/mL, and the change in impedance against the blank was recorded. Following this, the sensor was immersed in 1X PBS and subjected to ultrasound for 10 seconds. Subsequently, the impedance of the cTnI sensor exposed to blank and 0.50 pg/mL cTnI was recorded, and the impedance change was calculated.

Effect of ACEO on sensing performance

AC voltage was applied to two working electrodes with a function waveform generator (HP 33120A) to enhance the sensitivity of the cTnI sensor. This process involves the application of an alternating electric field to drive the movement of biofluids. The dependence of the applied AC voltage and duration on the binding of the cTnI on the sensor surface was investigated by exposing the sensor to cTnI at a concentration of 0.1 pg/mL and subjecting the electrodes to various voltages from 0 to 1.5 Vp-p at a frequency of 1 kHz for varying durations from 5 to 15 minutes. Subsequently, the impedance spectra were recorded, and the impedance change against the blank was calculated. Using an optimized applied voltage, the sensor was subjected to the blank repeatedly to evaluate the fluctuation in the impedance change due to ACEO. The cTnI sensors were exposed to different cTnI concentrations from 0.02 pg/mL to 1.5 ng/mL, prepared in 10% human serum with ACEO applied. The corresponding impedance spectra were recorded to obtain the impedance changes to quantify the sensitivity of the cTnI sensor enhanced by ACEO.

Sensing performance of the flexible cTnI sensor

We characterized the effect of bending on the baseline impedance magnitude of the cTnI sensor by measuring the impedance at 0.1 Hz in 1× PBS while the device was conformed to cylinders with radii ranging from 4.5 mm to 1.25 mm. The flexible sensors were exposed to varying concentrations of cTnI from 0.02 pg/mL to 1.5 ng/mL in artificial saliva. The corresponding impedance spectra were recorded to obtain impedance changes using the impedance in saliva without cTnI as a baseline. We applied the optimized AECO condition to the flexible cTnI sensor and evaluated the sensitivity enhancement due to AECO.

Results and Discussion

Design of the peptide-based electrochemical sensor

The electrochemical sensor comprises four electrodes, including two interdigitated working electrodes, one counter, and one reference electrode (Figure 1a). The four-electrode device was prepared with a standard microfabrication protocol, including gold thin film deposition and patterning with photolithography (see details in the experimental section). The gold surface of the reference electrode was coated with silver using electrochemical deposition and then treated with iron chloride to convert Ag to Ag/AgCl (Figure S1). The interdigitated electrodes are 20 μm in width and 20 μm in spacing. Figure 1b highlights the electrode functionalization, target detection, and sensor refreshing process. The interdigitated electrodes were functionalized with cTnI-specific peptide (sequence FYSHSFHENWPSC) through thiol-gold bonds. The human cTnI-binding peptide was originally identified via polyvalent phage display library screening(Park et al. 2010). This peptide has been validated in multiple biosensing studies for cTnI recognition, including electrochemical and plasmonic platforms(Tadepalli et al. 2015; Wu et al. 2010). The peptide is chosen as a biorecognition element because of its stability under diverse conditions, including elevated temperatures and harsh chemical environments(Tadepalli et al. 2015). All electrode surfaces were blocked with bovine serum albumin (BSA) to minimize nonspecific binding of interfering molecules onto the sensor surface. Electrochemical impedance measurements quantify the concentration of cTnI in biofluids. Subsequently, the captured cTnI can be removed from the sensor surface by ultrasonic cleaning at 40 kHz.

To achieve highly sensitive detection and quantification of cTnI, the interdigitated electrodes are designed to enhance the cTnI binding to the sensor surface through electroosmosis. This process involves the application of an alternating electric field to drive the movement of biofluids, including serum and saliva (Figure 1c). The electroosmotic flow enhances diffusion-limited analyte transport and concentrates target analytes near the sensor surface, leading to increased binding events. Previous work shows that electroosmosis can significantly enhance the binding of low-abundant molecular targets, therefore improving the sensor sensitivity (Ondevilla et al. 2022; Song et al. 2017).

cTnI sensor functionalization and characterization

We employed electrochemical impedance spectroscopy to characterize the sensor functionalization and quantify cTnI concentrations owing to its high sensitivity to surface molecular changes(Lazanas and Prodromidis 2023). EIS enables label-free and mediator-

free detection by directly probing changes in interfacial capacitance and dielectric properties induced by peptide-protein binding. For non-electroactive protein biomarkers such as cTnI, voltammetric techniques typically rely on redox mediators or electroactive labels to generate measurable Faradaic currents, which can complicate in situ operation and limit sensor refreshability. In contrast, EIS allows quantitative sensing directly in physiological buffers without additional reagents, making it well-suited for this refreshable, ACEO-enhanced sensing platform. The electrochemical impedance spectra of electrodes at frequencies from 0.1 to 10 kHz were recorded following surface modification and cTnI binding in phosphate-buffered saline (PBS). Figure 2a and 2b show the impedance magnitudes and phase angles following the peptide functionalization and cTnI binding. The electrode impedance magnitude decreases with increasing frequency from 0.1 Hz to 10 kHz. The impedance increased after the electrode was functionalized with cTnI-specific peptides and blocked with 3wt% BSA. The impedance increase is more significant at lower frequencies, consistent with impedance changes dominated by interfacial capacitive effects following biomolecular binding at the electrode surface(Katz and Willner 2003; Lisdat and Schäfer 2008). The Nyquist plot reveals the changes in the resistance (Zreal) and reactance (Zimag) of electrodes after each step (Figure 2c). Peptides and BSA created a barrier to electron transfer and increased charge transfer resistance, as shown in the Nyquist plot. In addition, biomolecules have a lower dielectric constant than PBS and increase the dielectric layer thickness at the electrolyte-electrode, resulting in a decreased double-layer capacitance and an increased capacitive reactance.(Li et al. 2013) After exposing the cTnI peptide-modified sensor to 1.5 ng/mL cTnI, the impedance increased, arising from concurrent changes in resistance and capacitance, with the reduction in interfacial capacitance dominating the low-frequency impedance response (Figure 2c). Fitting the impedance spectra with an equivalent-circuit model indicates that the impedance response to cTnI binding is dominated by changes in interfacial capacitive behavior, as reflected by a decrease in Y_0 and an increase in the CPE exponent α (Figure S2, Table S1). Although the fitted polarization resistance R_p increases, the real component of impedance at the readout frequency (0.1 Hz) decreases, indicating reduced effective interfacial resistance in the frequency regime relevant for sensing. Prior molecular dynamics simulations suggest that cTnI binding induces extension of the peptide from the gold surface into the solution(Tadepalli et al. 2015). The observed decrease in interfacial resistance may be associated with binding-induced interfacial reorganization, such as ion redistribution and rearrangement of the peptide layer, which can facilitate ionic transport at the electrode-electrolyte interface in non-Faradaic EIS systems.

We characterized the sensitivity, specificity, stability, and refreshability of the cTnI sensors to demonstrate their reliable performance. High sensitivity is important for accurate detection and quantification of cTnI at a low pg/mL concentration in complex body fluids, such as serum and saliva. We measured the electrochemical impedance at low frequency from 0.1 to 10 Hz after exposing the peptide functionalized sensor to varying concentrations of cTnI from 0 pg/mL to 1.5 ng/mL in 10% human serum after 5-minute incubation (Figure 2d). The tested cTnI concentrations span both physiological and pathological ranges(Antman Elliott et al. 1996; Thulin et al. 2023). The lower limit of detection (LOD) of high-sensitivity troponin I (hs-cTnI) assays typically falls between 0.7 and 3

pg/mL(Thulin et al. 2023). Clinical studies have demonstrated that patients with cTnI levels ≥ 0.4 ng/mL exhibit a significantly higher mortality rate compared with those having cTnI levels < 0.4 ng/mL(Antman Elliott et al. 1996). The impedance increased with increasing the cTnI concentration, following the formation of the target-peptide complex. The Nyquist plot shows the increased reactance and decreased resistance with increasing the cTnI concentration, highlighting the dominant effect of capacitance change due to the binding event. The impedance changes (Z_i-Z_{BL}) at 0.1 Hz yield a calibration curve to quantify the cTnI at concentrations from 0.02 pg/mL to 1.5 ng/mL (Figure 2e). We selected 0.1 Hz as the impedance readout frequency to ensure high sensitivity while maintaining reasonable measurement time and signal stability for point-of-care use. Z_i refers to the impedance magnitude for specific cTnI concentrations from 0.02 pg/mL to 1.5 ng/mL, and Z_{BL} refers to the impedance magnitude for the blank without cTnI. The impedance change increased following the increasing cTnI concentrations (Figure 2f). The LOD and limit of quantification (LOQ) were calculated to be 0.14 pg/mL and 3.7 pg/mL, respectively, lower than previous reports. The LOD was defined as the mean signal of the blank plus three times the standard deviation of the blank, and the LOQ was defined as the mean signal of the blank plus ten times the standard deviation of the blank. However, impedance change started to plateau at a concentration higher than 10 pg/mL, possibly due to the target depletion zone near the peptide.

Effect of AC electroosmosis (ACEO) on sensing performance

To expand the dynamic range and enhance the sensitivity, we employed AC electroosmosis to increase diffusion-limited cTnI transport and concentrate the target molecules near the sensor surface, thereby enhancing binding events. Electroosmotic flow was achieved by applying an alternating electric field to drive the movement of biofluids, effectively directing the target molecules toward the sensor surface. A controlled alternating electric field was produced by applying varying AC voltages at 1 kHz through two working electrodes. The selected frequency is based on previous work that reported the use of ACEO at 1 kHz as the optimal frequency for ultra-sensitive detection of cytokines in diluted serum(Song et al. 2017). We investigated the effect of the voltage amplitude and duration on the binding efficiency. The impedance change increased from 0.63 MΩ to 1.32 MΩ following the application of AC peak-to-peak voltages from 0.5 V to 1 V in the presence of 0.1 pg/mL cTnI for 10 minutes (Figure 3a). Further increasing the voltage to 1.5 V decreased the impedance change, possibly due to electrode degradation. The electrode surface could degrade when high voltage induces water electrolysis. To test the effect of time duration, we applied 1 V to induce ACEO for varying time durations from 5 to 15 minutes and measured the impedance change in response to 0.1 pg/mL cTnI. The impedance change increased with increasing ACEO time from 5 to 10 minutes, but did not further increase with 15 minutes (Figure 3b). Therefore, we chose 1 V for 10 minutes to induce ACEO to investigate the enhanced sensor sensitivity and dynamic range.

We exposed the sensor to various cTnI concentrations (0 pg/mL to 1.5 ng/mL) prepared in 10% human serum, followed by ACEO of 1 V for 10 minutes. Figure 3c shows the increased impedance with increasing cTnI concentrations in the frequency range from 0.1 to 10 Hz. Figure 3d shows the corresponding Nyquist plot, indicating that the dominant

change arises from the capacitance increase due to cTnI binding. The overall trend in the impedance changes is consistent with those without the application of ACEO, shown in Figure 2e. However, the impedance changes were much more enhanced in comparison with those without ACEO (Figure 3e). The impedance change increased by 5.2 times in response to 1.56 ng/mL cTnI, while it increased by 2.8 times in response to 0.1 pg/mL cTnI. It is important to confirm that the ACEO does not induce additional impedance change from nonspecific binding of molecules, considering enhanced molecular transport in complex biofluids. We exposed the sensor to 10% human serum without cTnI (blank) and measured the impedance change following an ACEO cycle 8 times (Figure 3f). The impedance change due to nonspecific binding and desorption is less than the change induced by 0.02 pg/mL cTnI. In addition, the device without peptide functionalization showed a similar level of nonspecific binding with ACEO, indicating these nonspecific changes were not associated with the presence of peptides (Figure S3). The low limit of detection (LOD) and low limit of quantification (LOQ) were calculated to be 0.031 pg/mL and 0.29 pg/mL, respectively, lower than previously reported electrochemical sensors and laboratory-based high-sensitivity assays. The lower LOD and LOQ compared to those without ACEO confirm that ACEO can effectively enhance the target binding and analytical sensitivity of the sensor.

We evaluated the specificity of the cTnI sensor by exposing it to common interfering molecules in circulating body fluids. We measured the impedance change induced by these molecules at physiologically relevant concentrations, including interleukin-6 (IL-6) of 7 pg/mL, tumor necrosis factor-α (TNF-α) of 25 pg/mL, and C-reactive protein (CRP) of 3 μg/mL (Figure 4a). The resultant impedance changes were below 150 kΩ, which is ~5-fold lower than that for 0.5 pg/mL cTnI, confirming the specificity of the cTnI sensor.

The sensor stability is important for reliable performance in resource-limited settings and wearable applications. We assessed the sensor's stability after incubation in 1X PBS at 37°C for varied time durations to simulate the in vivo body environment. The impedance change in response to 0.5 pg/mL cTnI remained consistent after storage from 1 to 4 days (Figure 4b). These results confirm the thermal stability of the peptide and sensor. We further challenged sensors with varying pH conditions from pH 3 to pH 11 to evaluate the pH stability. After exposing the sensor to different pH environments for 5 minutes, we measured the impedance change in response to 0.5 pg/mL cTnI (Figure 4c). The impedance change showed a negligible difference across the tested pH range, confirming the peptide's stability against highly acidic or alkaline conditions.

In addition to stability, the refreshability is important for achieving sensor reusability and enabling frequent monitoring of cTnI in situ. We tested the feasibility of dissociating the cTnI-peptide complexes with ultrasound to refresh the sensor. After the cTnIs were captured by the peptides, we exposed the sensor to ultrasound with acoustic power of ~250 mW/cm^2 at a frequency of 40 kHz for 10 seconds to refresh the sensor and recorded impedance in the blank. Figure 4d shows the impedance changes following exposure to 0.5 pg/mL cTnI, refreshing with ultrasound, and then exposure to the cTnI again for five cycles. After ultrasound refreshing, the impedance decreased to the blank baseline, fluctuating between 9.5 MΩ and 9.8 MΩ. After removing the baseline shift, the impedance change induced by 0.5 pg/mL cTnI binding remained 660 kΩ ± 42 kΩ after each refreshing

cycle (Figure 4e). In a control experiment, we fabricated the sensor without peptides, which showed an impedance change in response to 0.5 pg/mL cTnI, less than 90 kΩ (Figure S4). The small impedance change likely results from nonspecific binding of interfering molecules in serum. In comparison, the consistent impedance change of the cTnI sensor is much higher than that of the control, confirming that the cTnI-binding peptides remained stable on the sensor surface during ultrasound treatment. Figure 4f shows the average impedimetric response from 3 different sensors subjected to 5 cycles of ultrasonic cleaning. The consistent impedance changes validate the reproducible sensor response and refreshability. All experiments in Figure 4 were performed without ACEO to evaluate intrinsic sensor specificity, stability, and refreshability under baseline conditions. These results demonstrate that low-power ultrasound can regenerate the sensor by selectively disrupting noncovalent peptide-cTnI interactions without degrading the sensing interface. At the acoustic frequency and power used here (40 kHz, ~250 mW/cm^2), ultrasound primarily induces acoustic pressure oscillations and acoustic microstreaming in the surrounding liquid. These effects generate localized, transient interfacial agitation and fluid motion near the electrode-electrolyte interface, which are sufficient to accelerate dissociation of the weak noncovalent interactions while preserving chemisorbed Au-S bonds at the interface. While substantially extended regeneration cycling or higher acoustic power could eventually impact surface stability, systematic exploration of these operating limits will be pursued in future work.

Flexible sensor for saliva cTnI

Flexible, wearable sensors have strong potential for early diagnosis and continuous health monitoring in ambulatory or point-of-care settings(Heikenfeld et al. 2018; Mogera et al. 2022; Namkoong et al. 2022; Namkoong et al. 2024; Ray et al. 2019; Roy et al. 2024; Tian et al. 2019). Evidence from prior studies suggests that salivary cTnI holds promise as a noninvasive biomarker for the early diagnosis of acute myocardial infarction(Domenico et al. 2023). Accordingly, a flexible saliva sensor could enable seamless integration on a dental guard or along the internal surface of the mouth for real-time analysis of salivary cTnI. We fabricated the cTnI sensor on a 75 μm thin polyimide substrate following the same fabrication protocol of the cTnI sensor on the glass slides above (see details in the experimental section). Figure 5a illustrates the fabricated device wrapped around a glass rod, demonstrating its flexibility. The sensor has the same design and includes four well-defined electrodes, including a counter electrode, a reference electrode, and two interdigitated working electrodes (Figure 5b). The interdigitated working electrodes also have a width of 20 μm with 20 μm spacing between them. We characterized the effect of bending on the baseline impedance magnitude of the cTnI sensor by measuring the impedance at 0.1 Hz in 1X PBS while the device conformed to the cylinders with varying radii from 4.5 mm to 1.25 mm. As shown in Figure 5c, when the device was wrapped around cylinders with radii of 4.5 mm and 3 mm, the change in impedance is less than 5% compared to the impedance of the flat sensor. With further bending against cylinders with smaller radii of 2 mm and 1.25 mm, the impedance decreased by 20%. These results demonstrate that the impedance change is negligible when applying the sensor to the surface of a dental guard and the hard palate region, where the radius curvature is on a centimeter scale.

We tested the flexible sensor's performance by exposing the sensor to varying concentrations of cTnI, ranging from 0.02 pg/mL to 1.5 ng/mL, prepared in artificial saliva. Impedance spectra were recorded in the presence of the cTnI with and without ACEO. Figure 5d illustrates the impedance changes as the sensor was exposed to increasing concentrations of cTnI with ACEO for 10 minutes. As expected, the impedance increased with increasing cTnI concentrations. The ACEO effect on the sensitivity is highlighted in Figure 5e, which compares impedance change with and without ACEO. The results suggest that ACEO can effectively enhance the analytical sensitivity of the cTnI saliva sensor by ~3-fold. The LOD and LOQ of the sensor with ACEO enhancement were calculated to be 27 fg/mL and 60 fg/mL, showing the high sensitivity of this electrochemical biosensor. Figure 5f compares the LOD and sample incubation time of our sensor with previously reported electrochemical cTnI sensors. Notably, achieving an LOD below 1 pg/mL typically requires incubation times exceeding 10 minutes, which delays sensor response and hinders rapid cTnI quantification. In contrast, our sensor attains the lowest reported LOD with only a 10-minute sampling time, enabled by the implementation of ACEO.

Collectively, we demonstrated sensing in diluted human serum and artificial saliva to validate performance in complex biological matrices. However, we have not yet evaluated the sensor in undiluted serum, plasma, or whole blood. In these matrices, elevated ionic conductivity, nonspecific adsorption, and the presence of blood cells may influence low-frequency impedance measurements and ACEO-driven transport. Future work will address these challenges by incorporating size-selective or cell-excluding membranes, optimizing EIS excitation frequency and ACEO conditions, and implementing antifouling surface chemistries. These established strategies provide a clear pathway toward extending the platform to undiluted clinical samples.

Conclusions

In summary, we developed an electrochemical sensor employing a cTnI-binding peptide as the biorecognition element for sensitive, label-free, and mediator-free detection of cTnI. The sensor remains stable after exposure to extreme pH and physiological temperatures for several days. Integration of ACEO enhanced cTnI binding and analytical sensitivity, enabling detection down to 31 fg/mL in diluted serum and 27 fg/mL in artificial saliva. Importantly, the sensor can be reset using ultrasound, which removes bound targets without compromising the biorecognition element, thereby enabling reliable repeated quantification and prolonging sensor lifetime. The demonstrated sensitivity enhancement and refreshability can be broadly applied to other biosensing platforms with stable biorecognition elements, supporting the frequent detection of diverse biomarkers in body fluids and advancing early diagnosis and timely clinical intervention.

Supplementary Material

Refer to Web version on PubMed Central for supplementary material.

Acknowledgment

The authors acknowledge the funding from the National Institutes of Health (Grant No: R35GM147568) and the National Science Foundation (1648451). The device fabrication was conducted in the Texas A&M University AggieFab Nanofabrication Facility (RRID: SCR_023639), which is supported by the Texas A&M Engineering Experiment Station and Texas A&M University.

References

World Health Organization. Cardiovascular diseases (CVDs). https://www.who.int/news-room/fact-sheets/detail/cardiovascular-diseases-(cvds).

Antman Elliott M, Tanasijevic Milenko J, Thompson B, Schactman M, McCabe Carolyn H, Cannon Christopher P, Fischer George A, Fung Anthony Y, Thompson C, Wybenga D, Braunwald E, 1996. Cardiac-Specific Troponin I Levels to Predict the Risk of Mortality in Patients with Acute Coronary Syndromes. New England Journal of Medicine 335(18), 1342–1349. [PubMed: 8857017]

Apple FS, Jaffe AS, Sharkey S, Kavsak P, Kontos MC, Saenger AK, Smith S, 2017. Best Practices for Monitoring Cardiac Troponin in Detecting Myocardial Injury. Clinical Chemistry 63(1), 37–44. [PubMed: 28062607]

Cen S-Y, Ge X-Y, Chen Y, Wang A-J, Feng J-J, 2021. Label-free electrochemical immunosensor for ultrasensitive determination of cardiac troponin I based on porous fluffy-like AuPtPd trimetallic alloyed nanodendrites. Microchemical Journal 169, 106568.

Chekin F, Vasilescu A, Jijie R, Singh SK, Kurungot S, Iancu M, Badea G, Boukherroub R, Szunerits S, 2018. Sensitive electrochemical detection of cardiac troponin I in serum and saliva by nitrogen-doped porous reduced graphene oxide electrode. Sensors and Actuators B: Chemical 262, 180–187.

Das J, Gomis S, Chen JB, Yousefi H, Ahmed S, Mahmud A, Zhou W, Sargent EH, Kelley SO, 2021. Reagentless biomolecular analysis using a molecular pendulum. Nature Chemistry 13(5), 428–434.

Domenico T, Rita A, Giacomo S, Diego A, Thelma P, Mariana G, Giampaolo N, Francesco N, Maria G, Francesco F, Bruno B, Marco M, Diana C, 2023. Salivary biomarkers for diagnosis of acute myocardial infarction: A systematic review. International Journal of Cardiology 371, 54–64. [PubMed: 36167219]

Eshlaghi SN, Syedmoradi L, Amini A, Omidfar K, 2023. A Label-Free Electrochemical Aptasensor Based on Screen Printed Carbon Electrodes With Gold Nanoparticles-Polypyrrole Composite for Detection of Cardiac Troponin I. IEEE Sensors Journal 23(4), 3439–3445.

Feng S, Yan M, Xue Y, Huang J, Yang X, 2021. Electrochemical Immunosensor for Cardiac Troponin I Detection Based on Covalent Organic Framework and Enzyme-Catalyzed Signal Amplification. Analytical Chemistry 93(40), 13572–13579. [PubMed: 34591449]

Garg M, Guo H, Maclam E, Zhanov E, Samudrala S, Pavlov A, Rahman MS, Namkoong M, Moreno JP, Tian L, 2024. Molecularly Imprinted Wearable Sensor with Paper Microfluidics for Real-Time Sweat Biomarker Analysis. ACS Applied Materials & Interfaces 16(35), 46113–46122. [PubMed: 39178237]

Garg P, Morris P, Fazlanie AL, Vijayan S, Dancso B, Dastidar AG, Plein S, Mueller C, Haaf P, 2017. Cardiac biomarkers of acute coronary syndrome: from history to high-sensitivity cardiac troponin. Internal and Emergency Medicine 12(2), 147–155. [PubMed: 28188579]

Guo H, Yin Z, Namkoong M, Li Y, Nguyen T, Salcedo E, Arizpe I, Tian L, 2022. Printed Ultrastable Bioplasmonic Microarrays for Point-of-Need Biosensing. ACS Applied Materials & Interfaces 14(8), 10729–10737. [PubMed: 35171552]

Heikenfeld J, Jajack A, Rogers J, Gutruf P, Tian L, Pan T, Li R, Khine M, Kim J, Wang J, Kim J, 2018. Wearable sensors: modalities, challenges, and prospects. Lab Chip 18(2), 217–248. [PubMed: 29182185]

Katz E, Willner I, 2003. Probing Biomolecular Interactions at Conductive and Semiconductive Surfaces by Impedance Spectroscopy: Routes to Impedimetric Immunosensors, DNA-Sensors, and Enzyme Biosensors. Electroanalysis 15(11), 913–947.

Keller T, Hamm CW, 2019. High-sensitivity cardiac troponin assays: finally ready for prime time? Nature Reviews Cardiology 16(3), 135–136.

Keller T, Zeller T, Ojeda F, Tzikas S, Lillpopp L, Sinning C, Wild P, Genth-Zotz S, Warnholtz A, Giannitsis E, Mockel M, Bickel C, Peetz D, Lackner K, Baldus S, Munzel T, Blankenberg S, 2011. Serial Changes in Highly Sensitive Troponin I Assay and Early Diagnosis of Myocardial Infarction. Jama-J Am Med Assoc 306(24), 2684–2693.

Lazanas AC, Prodromidis MI, 2023. Electrochemical Impedance Spectroscopy—A Tutorial. ACS Measurement Science Au 3(3), 162–193. [PubMed: 37360038]

Li J, Zhang S, Zhang L, Zhang Y, Zhang H, Zhang C, Xuan X, Wang M, Zhang J, Yuan Y, 2021a. A Novel Graphene-Based Nanomaterial Modified Electrochemical Sensor for the Detection of Cardiac Troponin I. Front Chem 9, 680593. [PubMed: 34055747]

Li L, Li C, Zhang Z, Alexov E, 2013. On the Dielectric "Constant" of Proteins: Smooth Dielectric Function for Macromolecular Modeling and Its Implementation in DelPhi. Journal of Chemical Theory and Computation 9(4), 2126–2136. [PubMed: 23585741]

Li M, Wu Y, Ke C, Song Z, Zheng M, Yu Q, Zhu H, Guo H, Sun H, Liu M, 2024. An ultrasensitive unlabeled electrochemical immunosensor for the detection of cardiac troponin I based on Pt/Au–B,S,N-rGO as the signal amplification platform. Talanta 270, 125546. [PubMed: 38128282]

Li Y, Guo H, Yin Z, Lyle K, Tian L, 2021b. Metal–Organic Frameworks for Preserving the Functionality of Plasmonic Nanosensors. ACS Applied Materials & Interfaces 13(4), 5564–5573. [PubMed: 33496179]

Lisdat F, Schäfer D, 2008. The use of electrochemical impedance spectroscopy for biosensing. Analytical and Bioanalytical Chemistry 391(5), 1555–1567. [PubMed: 18414837]

Ma Y, Shen XL, Wang HS, Tao J, Huang JZ, Zeng Q, Wang LS, 2017. MIPs-graphene nanoplatelets-MWCNTs modified glassy carbon electrode for the determination of cardiac troponin I. Anal Biochem 520, 9–15. [PubMed: 28024754]

Mogera U, Guo H, Namkoong M, Rahman MS, Nguyen T, Tian L, 2022. Wearable plasmonic paper–based microfluidics for continuous sweat analysis. Science Advances 8(12), eabn1736.

Mokhtari Z, Khajehsharifi H, Hashemnia S, Solati Z, Azimpanah R, Shahrokhian S, 2020. Evaluation of molecular imprinted polymerized methylene blue/aptamer as a novel hybrid receptor for Cardiac Troponin I (cTnI) detection at glassy carbon electrodes modified with new biosynthesized ZnONPs. Sensors and Actuators B: Chemical 320, 128316.

Namkoong M, Guo H, Rahman MS, Wang D, Pfeil CJ, Hager S, Tian L, 2022. Moldable and transferrable conductive nanocomposites for epidermal electronics. npj Flexible Electronics 6(1), 41. [PubMed: 35996439]

Namkoong M, McMurray J, Branan K, Hernandez J, Gandhi M, Ida-Oze S, Cote G, Tian L, 2024. Contact Pressure-Guided Wearable Dual-Channel Bioimpedance Device for Continuous Hemodynamic Monitoring. Advanced Materials Technologies 9(3), 2301407. [PubMed: 38665229]

Negahdary M, Behjati-Ardakani M, Sattarahmady N, Yadegari H, Heli H, 2017. Electrochemical aptasensing of human cardiac troponin I based on an array of gold nanodumbbells-Applied to early detection of myocardial infarction. Sensors and Actuators B: Chemical 252, 62–71.

Ondevilla NAP, Wong T-W, Lee N-Y, Chang H-C, 2022. An AC electrokinetics-based electrochemical aptasensor for the rapid detection of microRNA-155. Biosensors and Bioelectronics 199, 113847. [PubMed: 34902642]

Park JP, Cropek DM, Banta S, 2010. High affinity peptides for the recognition of the heart disease biomarker troponin I identified using phage display. Biotechnology and Bioengineering 105(4), 678–686. [PubMed: 19891006]

Ray TR, Choi J, Bandodkar AJ, Krishnan S, Gutruf P, Tian L, Ghaffari R, Rogers JA, 2019. Bio-Integrated Wearable Systems: A Comprehensive Review. Chemical Reviews 119(8), 5461–5533. [PubMed: 30689360]

Roy S, Deo KA, Lee HP, Soukar J, Namkoong M, Tian L, Jaiswal A, Gaharwar AK, 2024. 3D Printed Electronic Skin for Strain, Pressure and Temperature Sensing. Advanced Functional Materials 34(22), 2313575.

Song Y, Chen P, Chung MT, Nidetz R, Park Y, Liu Z, McHugh W, Cornell TT, Fu J, Kurabayashi K, 2017. AC Electroosmosis-Enhanced Nanoplasmofluidic Detection of Ultralow-Concentration Cytokine. Nano Letters 17(4), 2374–2380. [PubMed: 28296413]

Szunerits S, Mishyn V, Grabowska I, Boukherroub R, 2019. Electrochemical cardiovascular platforms: Current state of the art and beyond. Biosensors and Bioelectronics 131, 287–298. [PubMed: 30851492]

Tadepalli S, Kuang Z, Jiang Q, Liu K-K, Fisher MA, Morrissey JJ, Kharasch ED, Slocik JM, Naik RR, Singamaneni S, 2015. Peptide Functionalized Gold Nanorods for the Sensitive Detection of a Cardiac Biomarker Using Plasmonic Paper Devices. Scientific Reports 5(1), 16206. [PubMed: 26552720]

Thulin IVL, Myrmel GMS, Jordalen SMF, Collinson P, Aakre K.M.J.J.o.L., Medicine, P., 2023. Point-of-care high-sensitivity troponin assays: advancements, clinical applications, and implementation considerations. Journal of Laboratory and Precision Medicine 8.

Thygesen K, Alpert JS, Jaffe AS, Chaitman BR, Bax JJ, Morrow DA, White HD, The Executive Group on behalf of the Joint European Society of Cardiology /American College of Cardiology / American Heart Association /World Heart Federation Task Force for the Universal Definition of Myocardial, 2018. Fourth Universal Definition of Myocardial Infarction (2018). Circulation 138(20), e618–e651. [PubMed: 30571511]

Tian L, Zimmerman B, Akhtar A, Yu KJ, Moore M, Wu J, Larsen RJ, Lee JW, Li J, Liu Y, Metzger B, Qu S, Guo X, Mathewson KE, Fan JA, Cornman J, Fatina M, Xie Z, Ma Y, Zhang J, Zhang Y, Dolcos F, Fabiani M, Gratton G, Bretl T, Hargrove LJ, Braun PV, Huang Y, Rogers JA, 2019. Large-area MRI-compatible epidermal electronic interfaces for prosthetic control and cognitive monitoring. Nature Biomedical Engineering 3(3), 194–205.

Tu D, Holderby A, Guo H, Mabbott S, Tian L, Coté GL, 2022. Spectrally multiplexed assay using gap enhanced nanoparticle for detection of a myocardial infarction biomarker panel. Analytica Chimica Acta 1198, 339562. [PubMed: 35190126]

Wang B, Jing R, Qi H, Gao Q, Zhang C, 2016. Label-free electrochemical impedance peptide-based biosensor for the detection of cardiac troponin I incorporating gold nanoparticles modified carbon electrode. Journal of Electroanalytical Chemistry 781, 212–217.

Wang XY, Zhang F, Zhang C, Zheng LR, Yang J, 2020. The Biomarkers for Acute Myocardial Infarction and Heart Failure. Biomed Res Int 2020.

Welsh P, Preiss D, Hayward C, Shah ASV, McAllister D, Briggs A, Boachie C, McConnachie A, Padmanabhan S, Welsh C, Woodward M, Campbell A, Porteous D, Mills NL, Sattar N, 2019. Cardiac Troponin T and Troponin I in the General Population. Circulation 139(24), 2754–2764. [PubMed: 31014085]

Westermann D, Neumann JT, Sörensen NA, Blankenberg S, 2017. High-sensitivity assays for troponin in patients with cardiac disease. Nature Reviews Cardiology 14(8), 472–483. [PubMed: 28383022]

Wu J, Cropek DM, West AC, Banta S, 2010. Development of a Troponin I Biosensor Using a Peptide Obtained through Phage Display. Analytical Chemistry 82(19), 8235–8243. [PubMed: 20831206]

Yin Z, Guo H, Li Y, Chiu J, Tian L, 2020. Ultrastable Plasmonic Bioink for Printable Point-Of-Care Biosensors. ACS Applied Materials & Interfaces 12(32), 35977–35985. [PubMed: 32677818]

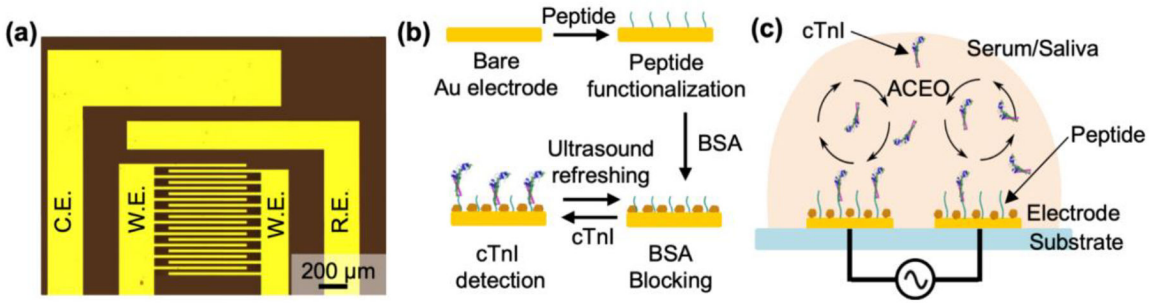

Figure 1.

Electrochemical cTnI sensor design. (a) Optical image of an electrochemical sensor consisting of interdigitated working electrodes (W.E.), counter (C.E.), and reference electrodes (R.E.). (b) Schematic illustration of electrode functionalization for cTnI quantification and ultrasound refreshing for removing the bound cTnI. (c) Schematic illustration of AC electroosmosis (ACEO)-enhanced cTnI binding on the sensor surface in serum and saliva.

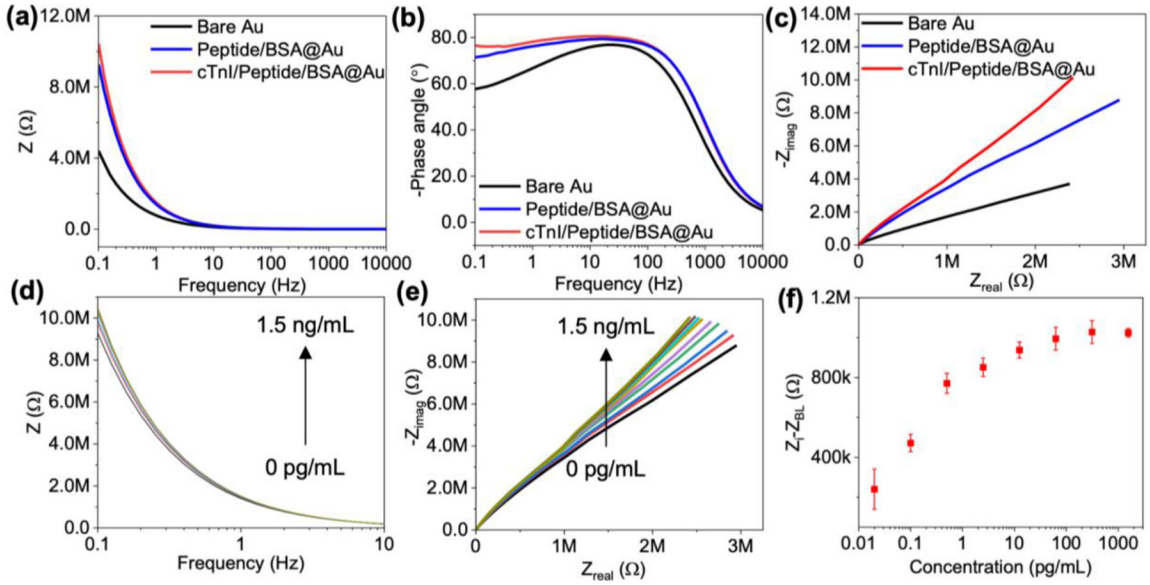

Figure 2.

Electrochemical sensor characterization. (a) Impedance response as a function of frequency for the bare electrode, peptide/BSA-modified electrode, and electrode after cTnI binding, and (b) corresponding phase angle plots. (c) Nyquist plots of bare electrode, peptide/BSA-modified electrode, and electrode after cTnI binding. (d) Impedimetric response to varying cTnI concentrations from 0 pg/mL to 1.5 ng/mL prepared in 10% human serum, and (e) corresponding Nyquist plots for different cTnI concentrations. (f) Increased impedance with increasing cTnI concentrations. Error bars in (f) represent the standard deviation of the measured values (n = 3).

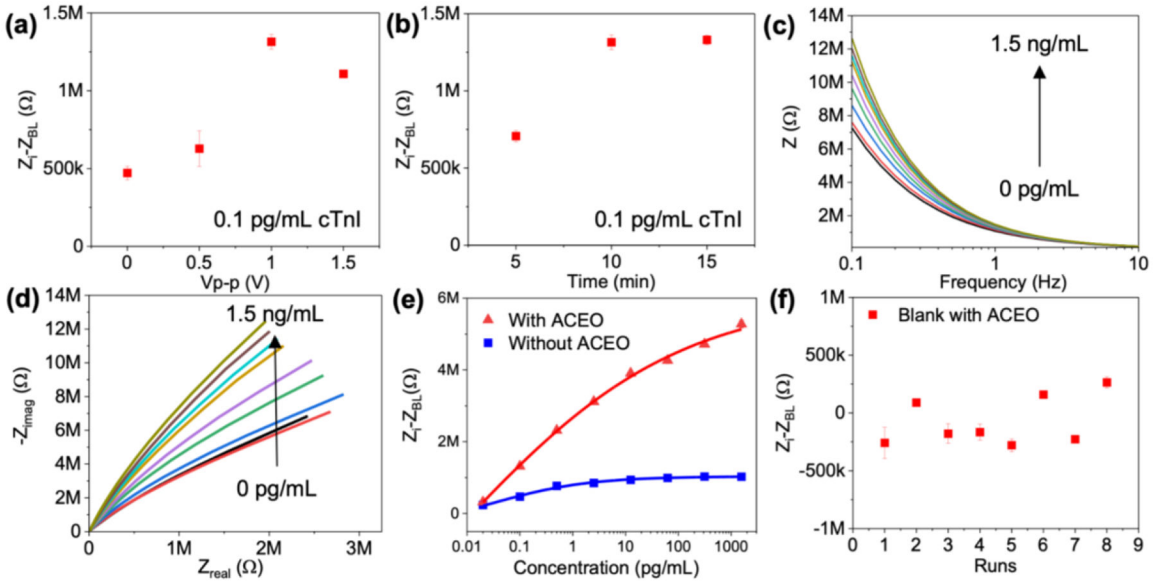

Figure 3.

ACEO-enhanced sensitivity. (a) Effect of different AC voltages during 10-minute ACEO treatment on the impedimetric change in response to 0.1 pg/mL cTnI. (b) Effect of ACEO duration at 1 V input on the impedimetric change in response to 0.1 pg/mL cTnI. (c) Impedimetric responses to varying cTnI concentrations (0 pg/mL to 1.5 ng/mL) with ACEO enhancement, and (d) the corresponding Nyquist plots. (e) Comparison of impedance changes with increasing cTnI concentrations in the presence and absence of ACEO. (f) Impedance fluctuations of the sensor in response to repeated ACEO treatment when exposed to the blank control (10% human serum without cTnI). Error bars in (a, b, e, f) represent the standard deviation of the measured values (n = 3).

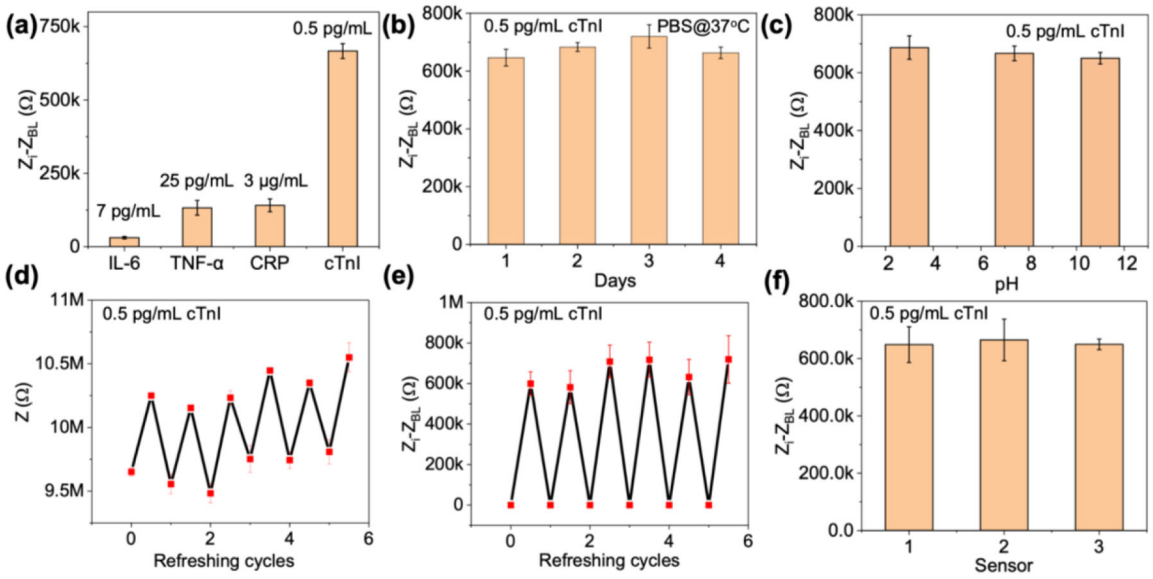

Figure 4.

Sensor selectivity, stability, and refreshability. (a) Impedance changes upon sensor exposure to interfering molecules compared to cTnI. (b) Impedance response to 0.5 pg/mL cTnI after exposure to varying pH conditions. (c) Impedance response to 0.5 pg/mL cTnI after storage in 1× PBS at 37 °C. (d) Impedance response after repeated exposure to 0.5 pg/mL cTnI followed by 10-second ultrasound refreshing, and (e) the corresponding impedance changes. (f) Averaged impedimetric responses over five ultrasound refreshing cycles for three sensors. Error bars in (a, b, c, d, e, f) represent the standard deviation of the measured values (n = 3).

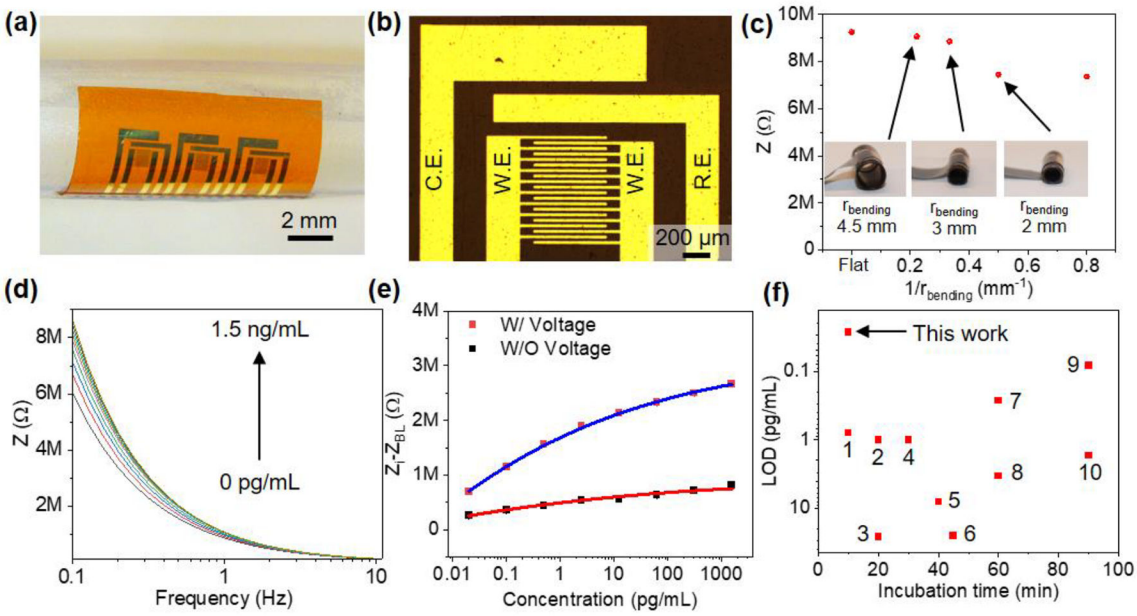

Figure 5.

Flexible electrochemical sensor. (a) Image demonstrating the bendability of the flexible electrochemical sensor. (b) Optical image of the sensor fabricated on a flexible polyimide substrate. (c) Impedimetric response of the flexible sensor as a function of radius of curvature. (d) Impedimetric responses to varying cTnI concentrations (0 pg/mL to 1.5 ng/mL) in artificial human saliva with ACEO treatment. (e) Comparison of sensor sensitivity with and without ACEO. (f) Comparison of the limit of detection (LOD) and sample incubation time from this work with literature reports on electrochemical detection of cTnI. Error bars in (c, e) represent the standard deviation of the measured values (n = 3).